Preclinical Development

Molecular Cancer Therapeutics

Pharmacodynamic Evaluation of the Target Efficacy of SB939, an Oral HDAC Inhibitor with Selectivity for Tumor Tissue

Veronica Novotny-Diermayr[1], Nina Sausgruber[1], Yung Kiang Loh[1], Mohammed Khalid Pasha[1], Ramesh Jayaraman[1], Hannes Hentze[1], Wei-Peng Yong[2], Boon-Cher Goh[2], Han-Chong Toh[3], Kantharaj Ethirajulu[1], Joy Zhu[1], and Jeanette Marjorie Wood[1]

Abstract

SB939 is an oral histone deacetylase (HDAC) inhibitor currently in phase II clinical trials potently inhibiting class I, II, and IV HDACs with favorable pharmacokinetic properties, resulting in tumor tissue accumulation. To show target efficacy, a Western blot assay measuring histone H3 acetylation (acH3) relative to a loading control was developed, validated on cancer cell lines, peripheral blood mononuclear cells (PBMC), and in animal tumor models. Exposure of cells to 60 nmol/L (22 ng/mL) SB939 for 24 hours was sufficient to detect an acH3 signal in 25 μg of protein lysate. AcH3 levels of liver, spleen, PBMCs, bone marrow and tumor were measured in BALB/c mice, HCT-116 xenografted BALB/c nude mice, or in SCID mice orthotopically engrafted with AML (HL-60) after oral treatment with SB939. AcH3 could only be detected after treatment. In all tissues, the highest signal detected was at the 3-hour time point on day 1. On day 15, the signal decreased in normal tissues but increased in cancerous tissues and became detectable in the bone marrow of leukemic mice. In all tissues, acH3 correlated with SB939 dose levels ($r^2 = 0.76$–0.94). When applied to PBMCs from 30 patients with advanced solid malignancies in a phase I clinical trial, a dose-dependent (10–80 mg) increase in relative acH3 was observed 3-hour postdose on day 1, correlating with C_{max} and AUC of SB939 concentrations in plasma ($r = 0.97$, $P = 0.014$). Our data show that the favorable pharmacokinetic and pharmacodynamic properties of SB939 are translated from preclinical models to patients. *Mol Cancer Ther; 10(7); 1207–17. ©2011 AACR.*

Introduction

Acetylation of core-histones and nonhistone proteins, such as transcription factors, nuclear receptors, structural proteins and chaperone proteins, is regulated by histone deacetylases (HDAC) and histone acetyltransferases (refs. 1–4). Numerous HDAC or histone acetyltransferase defects, leading to abnormal protein acetylation, were identified in hematological tumors or epithelial cancers, for example, mutation, translocation, amplification, or over-expression of CBP, p300, TIF-2, RARα, HDAC1, 2, and 3 (3, 5, 6). HDACs, therefore, have been postulated as targets for drug inhibition to restore normal acetylation of HDAC substrates and arrest tumor growth. Accumulation of acetylated proteins through HDAC inhibition leads to several cell-type–dependent responses, for example, differentiation, induction of cell-cycle arrest, apoptosis, and altered gene expression patterns (3, 7). This concept has now been validated with market approvals for the HDAC inhibitors (HDACi). SAHA (Vorinostat, Zolinza) and Romidepsin (Istodax) to treat cutaneous T-cell lymphoma (8, 9).

SB939 is an oral, hydroxamic acid–based HDACi currently in phase II clinical trials, potently inhibiting class I, II, and IV HDACs. In contrast to the registered compounds and other HDACi currently in clinical trials (10), SB939 has improved pharmaceutical and pharmacokinetic properties, resulting in high oral bioavailability and accumulation in tumor tissue (11).

Methods used to detect target efficacy for HDACi varied widely. An ELISA of histone extracts isolated from peripheral blood mononuclear cells (PBMC) was used to measure histone H3 acetylation (acH3) in clinical trials with SAHA (12). Measurements of HDAC enzyme inhibition in a fluorogenic whole cell HDAC enzyme assay (13), quantitative fluorescence-activated cell sorting for acetylated H2B or H3 in patients with hematological malignancies (14), or immunocytochemical detection of

Authors' Affiliations: [1]S*BIO Pte. Ltd., 1 Science Park Rd, The Capricorn, Singapore Science Park II; [2]Department of Hematology-Oncology, National University Hospital of Singapore; and [3]Medical Oncology, National Cancer Center, Singapore

Note: Supplementary material for this article is available at Molecular Cancer Therapeutics Online (http://mct.aacrjournals.org/).

Corresponding Author: Veronica Novotny-Diermayr, S*BIO Pte. Ltd., 1 Science Park Rd, #05–09 The Capricorn, Singapore Science Park II, Singapore 117528. Phone: 65-6827-5052; Fax: 65-6827-5005; E-mail: veronica_diermayr@sbio.com

doi: 10.1158/1535-7163.MCT-11-0044

acH3 in PBMCs (15) were used. Most techniques had shortfalls, especially high background acetylation in non-treated samples or low sensitivity. Here we describe a sensitive Western blot assay to detect histone H3 acetylated on Lysine 9 and 14, that detects dose-dependent HDACi. After testing on cultured cells and in mouse tumor models, it was applied to analyze target efficacy of SB939 in PBMCs from patients with advanced solid malignancies.

Materials and Methods

Compounds

SB939 hydrochloride salt was used *in vitro* and *in vivo* as described previously (11), for structure see Supplementary Fig. 1.

Cells

Cell lines [HCT-116 (ATCC-CCL247), HL-60 (ATCC-CCL-240), RAMOS (ATCC-CRL-1596)], used between passage 3 and 9 were obtained from the American Type Culture Collection, cultivated according to the vendor's instructions, tested for mycoplasma contamination (Mycoplasma *Plus* PCR Primer Set, Stratagene; Agilent Technologies Inc) and verified by STR profiling (John Hopkins University, MD). Human PBMCs were purified from venous blood drawn into BD Vacutainer CPT-tubes (Becton, Dickinson and Company), according to the manufacturer's instructions, and after washing with PBS, were maintained in RPMI 1640 containing 10% FBS (Invitrogen Corporation). Subsets of human PBMCs were isolated by magnetic cell sorting using MACS-beads (Miltenyi Biotec GmbH, Bergisch Gladbach, Germany, see Supplementary data). Murine PBMCs were prepared as described recently (11).

Lysis and Western blot assay

Cell lysis, protein quantification and Western blots were conducted as described previously (11). To compare patient samples across different Western blot membranes, 25 μg of RAMOS cell lysate, treated with dimethyl sulfoxide (DMSO; negative control), or with 2 μmol/L SB939 (positive control) for 24 hours were included on every Western blot. For animal studies, the highest value in each blot was set to 100% (for each data set) and the percentage of acetylation of the other data points was calculated to show all replicas in 1 figure. Statistical analyses were conducted in GraphPad Prism 5 (GraphPad Software).

Animal models

Female BALB/c mice and athymic BALB/c nude mice (BALB/cOlaHsd-*Foxn1*^{nu}) were 10 to 16 weeks of age; female SCID mice (C.B.-17/IcrHanHsd-*Prkdc*^{scid}) 5 to 11 weeks of age, all from Biological Resource Centre (BRC, Biopolis, Singapore). Standard protocols were followed, in compliance with the NIH and NACLAR guidelines (IACUC approval #0800371).

The colorectal cancer model (HCT-116) was conducted as described previously (11). Drug treatment started at a mean tumor volume of about 200 mm^3.

For the orthotopic leukemia model, SCID mice were injected i.v. with 10×10^6 HL-60 cells in 100 μL serum-free medium. Mice were checked for signs of paralysis 3×/week. An additional take-rate control group ($n = 3$) was tested for human cells in different tissues (see Supplementary data) on day 29 and found to have about 35% of bone marrow and about 10% of blood cells staining positive for cell surface markers of HL-60 cells, indicating a good take-rate. Treatment of the experimental group started on day 30 after inoculation (before the first mouse showed symptoms of paralysis).

SB939 (125 mg/kg) was administered by oral gavage in a 3×/wk schedule for up to 15 days. Mice were sacrificed on day 1 and day 15, before drug administration (predose) and 3, 8, or 24 hours after dosing. Tissues were harvested from at least 3 mice per time point, analyzed by Western blotting followed by densitometry. To determine dose–response, animals were dosed once with 25 to 200 mg/kg orally and mice were sacrificed after 3 hours. Tissues were snap-frozen in liquid nitrogen, with the exception of PBMCs, which were lysed directly after extraction.

Pharmacokinetic analysis of SB939

Plasma levels of SB939 in human or murine plasma were measured at MPI Research (Mattawan; ref. 16), or determined as previously described (11), respectively.

Patient samples and treatment

Thirty-one patients were enrolled, 1 patient withdrew consent before dosing. PBMCs were collected from the remaining 30 patients, treated with the following doses (n): 10 mg (3), 20 mg (3), 40 mg (8), 60 mg (10), and 80 mg (6) and evaluated for acH3. SB939 was administered orally every Monday, Wednesday, and Friday, for 21 days, followed by 7 days of rest, see (16) for trial design and patient characteristics.

PBMCs, obtained from 8 mL venous blood of consented patients under IRB-approved protocols, were snap-frozen in liquid nitrogen after isolation on day 1 and day 15 at predose, 3 or 24 hours post dose. A PBMC pellet and sufficient protein to detect β-actin under standardized conditions at an exposure of 100 s (at normal sensitivity) in a Luminescent Image Analyzer (LAS-3000, Fujifilm) was present in samples from all 30 patients. Two samples of the 80 mg cohort and 2 day 1 samples from the 60 mg cohort had to be excluded due to technical reasons. Three single values (all day 15, predose or 3 hours, Supplementary Table S2) were excluded from the statistics using Grubb's test for outliers (GraphPad Software).

Results

Protein requirement for signal detection

Three micrograms of protein lysate from either HCT-116 or HL-60 cells, treated for 24 hours with 2 μmol/L

SB939, were sufficient to obtain a strong acetylation of K9 and K14 of histone H3 (Fig. 1A left). With enhanced contrast, as little as 0.4 μg were enough to detect acH3 in the more HDACi-sensitive HL-60 liquid tumor cell line, and 1.6 μg in the less sensitive HCT-116 solid tumor cell line (Fig. 1A right). This Western blot assay, established after testing 6 different acH3 antibodies (Supplementary Fig. S2), was reproducible across different batches of cells, even after several freeze thaw cycles (data not shown).

Limits of Detection

The lowest concentration of SB939 leading to acH3 was 22 ng/mL (0.06 μmol/L) for both HCT-116 and HL-60 cells treated for 24 hours with SB939. In HL-60 cells, maximal acH3 levels were reached at 1 μmol/L SB939 not increasing further after treatment with 2 μmol/L. In contrast, in HCT-116 cells, the signal intensified further from 1 to 2 μmol/L, but was overall lower than in the HL-60 cell line. Notably, no background signal was detected for DMSO-treated cells, even after enhanced contrast settings (Fig. 1B). A dose-dependent increase in acH3 signal was also observed using freshly isolated PBMCs from healthy volunteers treated with SB939 *ex vivo*. The minimal SB939 concentration required to elicit a strong acH3 signal was 88 ng/mL (250 nmol/L), with a faint signal detected after exposure to 44 ng/mL (125 nmol/L; Fig. 1C), showing that the assay is sufficiently sensitive to detect acH3 in solid and liquid tumor cell lines and in normal PBMCs after exposure to low-nanomolar concentrations of SB939 without background for nontreated cells.

AcH3 signal in different subsets of human PBMCs

Because PBMCs are a mixed population of T cells, B cells, monocytes, and natural killer cells, the individual cell populations contributing to the acH3 signal detected in SB939-treated PBMCs were determined after cell sorting with antibodies against lineage-specific cell surface proteins. $CD20^+$ B-lymphocytes showed highest acH3 levels, followed by much lower acH3 levels in $CD3^+$ T-lymphocytes and lowest acetylation levels in $CD16^+$ monocytic cells (Fig. 1D). Therefore, acH3 levels in PBMCs after treatment with an HDACi might not be directly comparable across patients, particularly in patients with leukemic malignancies with abnormal percentages of myeloid, lymphoid, or monocytic cells.

Pharmacodynamic evaluation in normal BALB/c mice

To ensure that solid tumor patient's PBMCs would be a useful surrogate tissue to assess target efficacy of SB939, PBMCs and tissues from normal BALB/c mice were analyzed after a single dose or after 15 days of treatment with SB939 (125 mg/kg, 3×/wk; representing the clinical schedule used in the phase I study). AcH3 was detected in 25 μg lysate of all tissues (Fig. 2A), with the exception of bone marrow where no signal could be detected even in combined lysates from 3 mice (75 μg, data not shown). In liver and spleen, the highest acH3 signal was observed on day 1 at the 3-hour time point in all animals. On day 15, the highest signal was also at 3 hours, however, the signal on day 15 was weaker than the signal on day 1 for all tissues including PBMCs (Fig. 2A, compare 2nd column and 6th column). For PBMCs, the highest acH3 signal on average was at 8 hours on day 1, but individual animals showed considerable variation. In liver and spleen tissue, acH3 could not be detected at 24 hours on day 1, whereas on day 15 there was a signal detectable showing a more sustained target inhibition after chronic treatment (Fig. 2A). Plasma samples, analyzed concurrently for SB939 concentrations, showed that the highest plasma concentrations (C_{max}) on day 1 were at 3 hours (mean 147 ng/mL), falling to 48 ng/mL at 8 hours. On day 15, the mean C_{max} at 3 hours was 330 ng/mL, falling to 46 ng/mL at 8 h and 4.9 ng/mL at 24 hours (Fig. 2B). The time point with the highest C_{max} coincided with the time point where highest acH3 signals were observed, indicating concentration dependency of the acH3 signal.

Pharmacodynamic evaluation in a solid tumor model

To determine the effects of SB939 on its molecular target in normal versus tumor tissue, tissues were collected and analyzed from a mouse model of a human solid tumor (HCT-116 colorectal cancer cells grown *s.c.* in nude mice) after a single dose, or 15 days of treatment with SB939 (125 mg/kg., 3×/wk). As observed in nontumor-bearing mice, no signal was detected in bone marrow (data not shown). In other nontumor tissues (liver, spleen, and PBMCs) highest acH3 signals were detected on day 1 at the 3-hour time point, whereas in the tumor tissue the highest signal was on day 15 at 3 hours, indicating that the SB939-induced acH3 signal decreased over time in healthy tissue but increased in tumor tissue (Fig. 3A and B, compare first 3 and right most). Similar to the experiment in normal mice, the acH3 signal in all tissues of the tumor-bearing mice was slightly prolonged on day 15, with stronger signals at 8 and/or 24 hours on day 15 compared with day 1. The background signals in vehicle-treated or predose samples from day 1 were negligible (Fig. 3A and B). In PBMCs, the trend was the same as for other healthy tissues; on average the highest signal was observed on day 1 at 3 hours, but on day 15 the time point showing the highest acH3 signal was different for each animal (either at predose, 3 or 8 hours). Highest plasma concentrations of SB939 measured in BALB/c nude mice averaged 193 ng/mL (at the 3-hour time point on day 1) and 177 ng/mL at the same time point on day 15, decreasing to 35 and 45 ng/mL, respectively at 8 hours (Fig. 3C).

Pharmacodynamic evaluation of SB939 in a liquid tumor model

To investigate whether acH3 levels would also increase in liquid tumor cells, tissues were harvested on day 1 and day 15 from SCID mice injected with HL-60 human

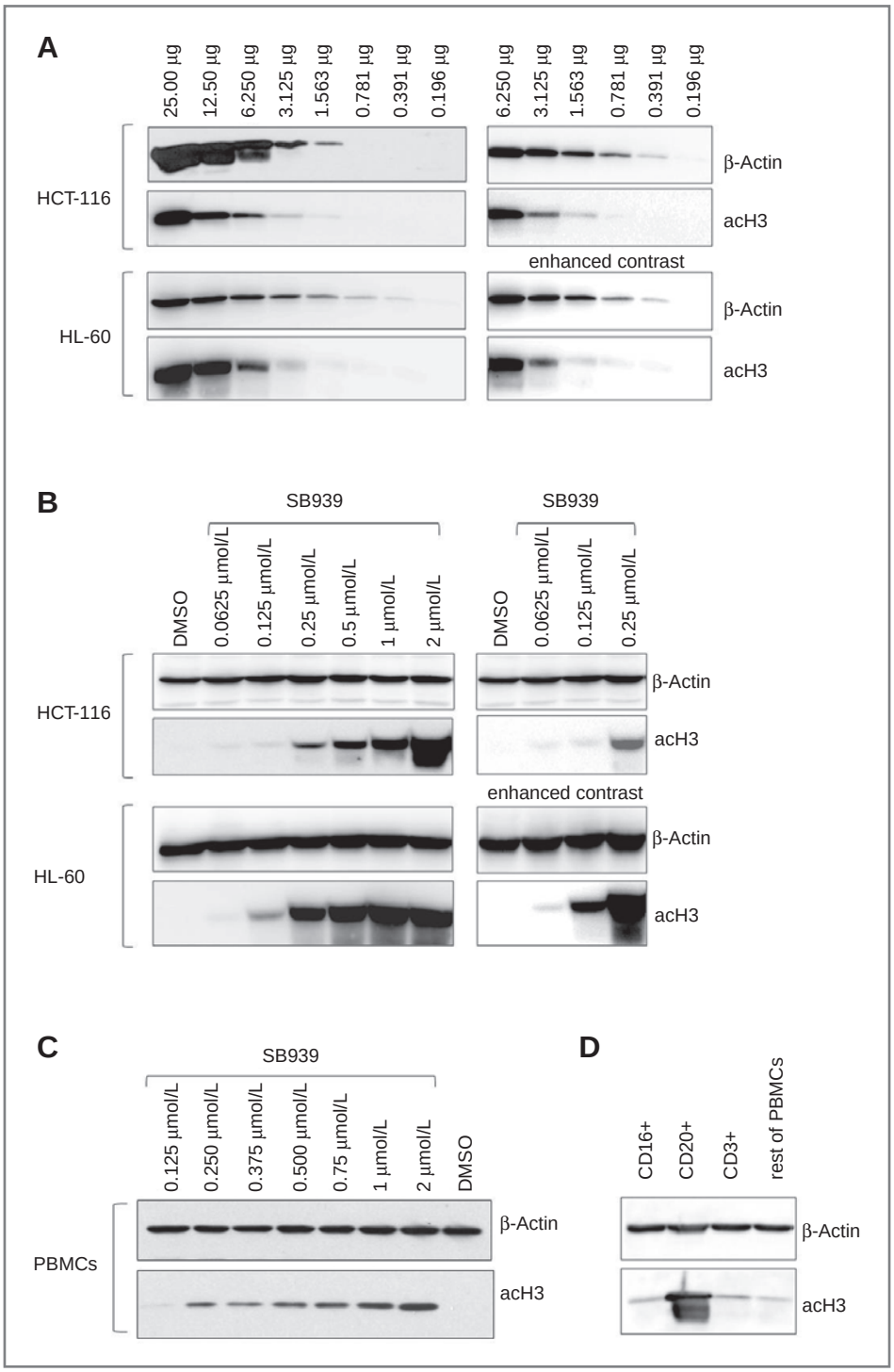

Figure 1. Limits of detection of acetylated (K9/K14) histone H3. Western blot analysis of cells treated with SB939 for 24 hours. All blots shown are one of at least 3 independent experiments carried out. Antibodies used are indicated on the right. A, the minimum amount of protein lysate necessary to detect acH3 in HCT-116 or HL-60 cells, with enhanced contrast settings for parts of the left shown on the right. B and C, the minimum concentration of SB939 required for detection after a 24-hour treatment in cell lines or human PBMCs. D, human PBMCs were positively sorted for cell surface antigens (as indicated), with 25 µg protein/sample analyzed.

promyelocytic leukemia cells after treatment with SB939 (125 mg/kg, 3×/week). In healthy tissues (liver and spleen), the highest relative acetylation signals were again measured at the 3-hour time point on day 1 and although the acH3 levels were prolonged on day 15, they were only a maximum of 40% of the values at 3-hour on day 1 (Fig. 4A). In contrast, in diseased tissues, the relative acH3 signals were higher on day 15 than on day 1. In the bone marrow of diseased mice, with an average of 35% positive staining for a cell surface marker of HL-60 AML cells (CD4 and/or HLA-ABC; data not shown), acH3 was detectable 3-hour postdose on day 15 (see Fig. 4A). In the 2 other animal models tested with no disease in the bone marrow, there was no detectable acH3

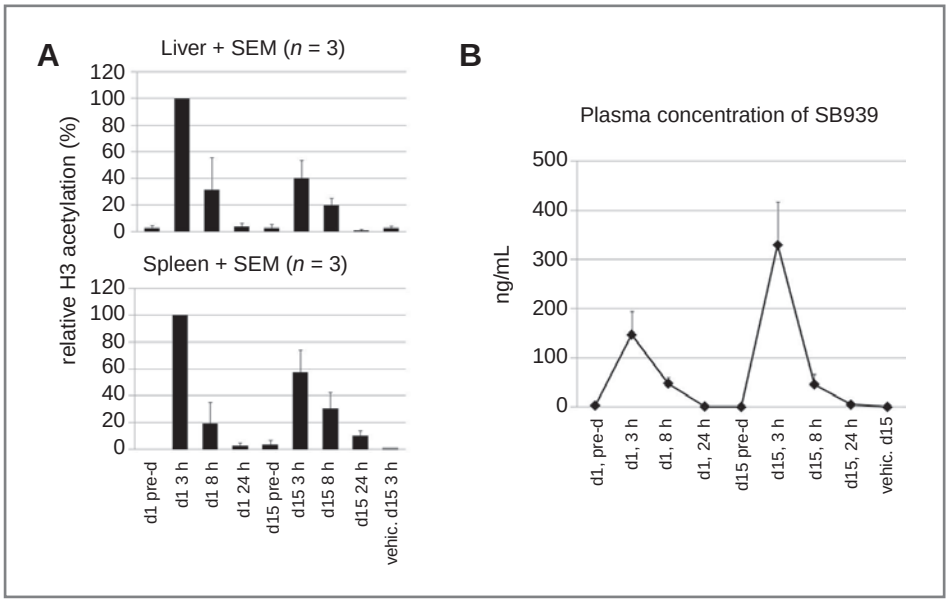

Figure 2. Biomarker validation in BALB/c mice. BALB/C mice were dosed with 125 mg/kg SB939 for 15 days, 3×/week. Three animals each were euthanized at the indicated time points. A, tissues were lyzed, Western blots were conducted, and normalized acH3 values were calculated (see Material and Methods). Densitometric analyses from 3 Western blots each were combined for 1 graph SB939 plasma concentration (±SD) from the same mice (B). pre-d, predose.

signal in the bone marrow. In PBMC from leukemic mice, containing up to 16% of leukemic cells (data not shown), the highest acH3 signals were observed on day 15, either at 3 or at 24 hours postdose, showing that SB939 treatment also led to enhanced acH3 signal in liquid tumor tissue. Plasma concentrations of SB939 in leukemic mice were significantly higher at 3 hours postdose on day 15 compared with naive SCID mice (910 ± 289 ng/mL compared with 292 ± 34 ng/mL in naive mice, $P < 0.001$) after the same dose of SB939 (Supplementary Table S1), likely an effect of decreased SB939 liver metabolism, due to increased lymphocytes (data not shown). In conclusion, SB939 led to rapid acetylation of histone H3 in tissues, which after chronic treatment decreased in healthy tissue, but increased in tumor tissue.

Dose response in normal and tumor tissues

To establish the dose dependency of the acH3 signal in different tissues, mice were treated with doses from 25 to 200 mg/kg SB939 and sacrificed 3 hours postdose. Because acH3 signals of B and T cells are very different (Fig. 1C) and nude mice are deficient in T-cells, only BALB/c mice were used to show dose dependency of the response in PBMCs. HCT-116–xenografted nude mice were used to show the dose–response in tumor tissue. In all tissues analyzed, acH3 signals increased dose dependently (Fig. 5A and B). In liver tissue, doses from 25 to 50 mg/kg led to dose-dependent and significant ($P < 0.5$) increases in acH3. The acH3 signal was saturated at dose levels of 125 and 100 mg/kg in liver and tumor tissues, respectively. A further increase in SB939 concentration did not lead to a further increase in acH3 levels in liver or tumor tissue (Fig. 5A and B). PBMCs of BALB/c mice showed the least dose sensitivity, with a maximal acH3 signal of about 70% at 150 mg/kg. The highest absolute acH3 values and the earliest saturation of the signal (at 100 mg/kg) were observed in tumor tissue, further indicating selectivity of SB939 for tumor tissue over normal tissue.

AcH3 signal increased dose dependently in PBMCs from solid tumor patients treated with SB939

The established Western blot assay was used to detect acH3 in PBMCs from solid tumor patients from a phase I trial. Samples from 30 patients were analyzed at 6 timepoints each: predose, 3 and 24 hours postdose on day 1 and day 15. The 3 hours postdose sampling point was close to the time where maximal concentrations of SB939 were observed in the plasma (T_{max}) at an average of 1.45 ± 1.0 1 hour (from 0.5 to 4 hours across all dose levels on day 1 and day 15 combined; individual patient's data not shown), with the dosage of C_{max} of SB939 increasing proportionally (16). AcH3 was detectable with highest levels either at 3 or 24 hours postdose in 2/3 samples from the 10 mg cohort (Supplementary Table S2) and a SB939 C_{max} of 39 ± 16 ng/mL. The 10 mg patient without detectable acH3 levels had lower plasma levels of SB939 than the other 2 patients, with the area under the (concentration-time) curve ($AUC_{0-\infty}$) being 171 ng/h/mL compared with 240 and 275 ng/h/mL, respectively, for the remaining 2 patients (data not shown). For the 3 patients, dosed with 20 mg (C_{max} 61 ± 46 ng/mL), acH3 signals could be detected in PBMCs from all patients, with the highest relative acH3 levels on day 15 at 3 hours postdose being 0.8 (Fig. 6A, top). Eight patients were treated with 40 mg and 10 patients treated with 60 mg SB939, with C_{max} of 158 ± 101 and 178 ± 102 ng/mL, respectively, for the 40 and 60 mg cohorts. The maximal acH3 signals obtained from these samples were 1 and 1.35, respectively (at 3 hours on day 1). At 60 mg/kg, the difference between predose levels and 3 hours postdose levels was significant ($P = 0.0265$; Fig. 6A, bottom);

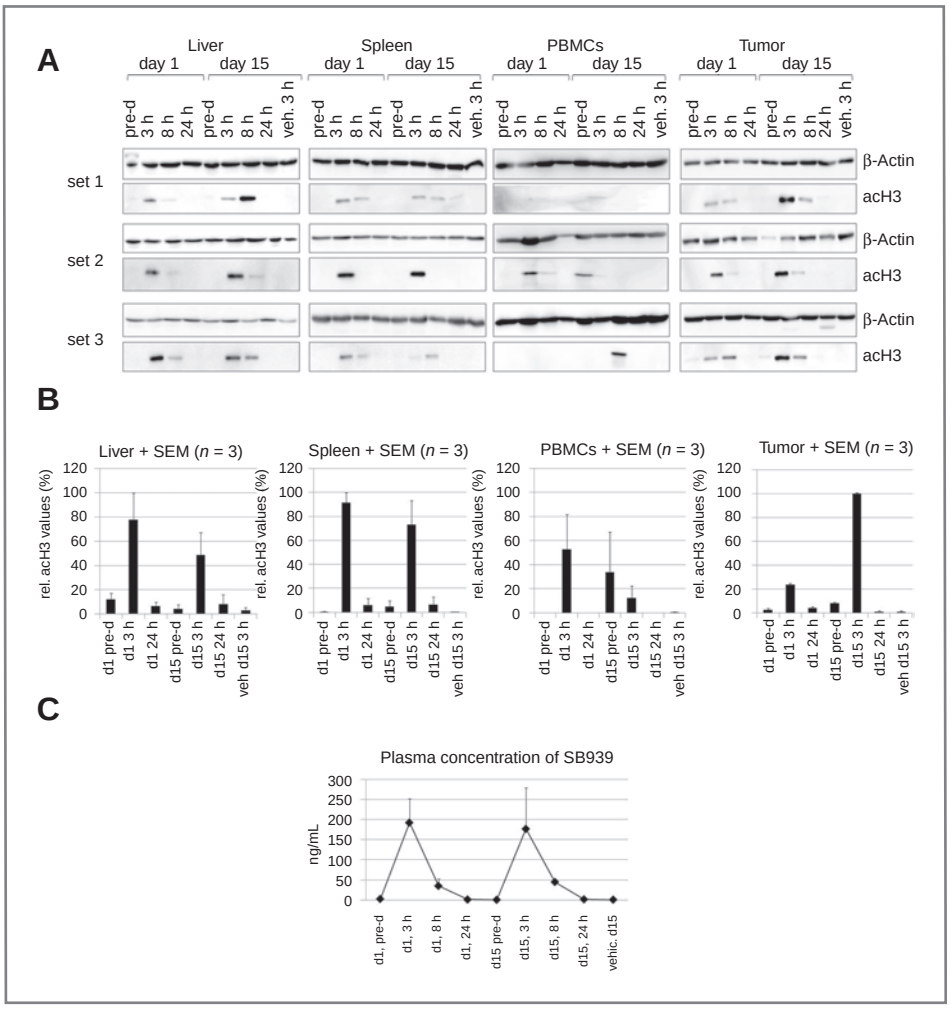

Figure 3. Acetylation of histone H3 decreased in normal tissues but increased in HCT-116 xenograft tissue after prolonged treatment. HCT-116–xenografted nude mice were dosed with 125 mg/kg SB939 3×/wk for 15 days. A, 3 animals each were euthanized at the time point indicated, Western blots shown. B, densitometric analysis for all time points (except 8 hours). Graphs were prepared as described for Fig. 1C. SB939 plasma concentration (±SD) was from the mice used. pre-d, predose.

individual Western blots for all complete samples (i.e., samples collected at all 6 time points) of the 60 mg dose level are shown in Fig. 6B. The highest acH3 signal was at 3 hours on day 1, with the exception of patient 505 and 503, where the strongest acH3 signal was detected at 3 hours on day 15. Of the 6 patients treated with 80 mg, only 4 were evaluable for pharmacodynamic analysis on day 1 (average maximal acetylation of 2.02). On day 15, the highest acH3 value was 0.16 for 2 evaluable patients, not allowing statistical evaluation (individual acH3 values in Supplemental Table S2). A positive correlation between the $AUC_{0-\infty}$ for the 5 dose levels and the maximal acH3 values was observed (Pearson $r = 0.97$, $P = 0.014$) and described elsewhere (16). The average C_{max} for each dose level also positively correlated with the average maximal acH3 levels (Pearson $r = 0.80$, $P = 0.04$), see Fig. 6C.

Of 30 patients, 8 had stable disease and 3 had a minor response. Interestingly, 2 of the 3 responders showed the greatest acH3 response observed across patients (7.6 and 6.1, respectively, Fig. 6D). One was a non–small cell lung cancer (NSCL) patient (1% tumor shrinkage) who withdrew consent after 31 days on the study and the other was with olfactory neuroblastoma (patient 505) who completed 12 cycles (maximum 18.4% tumor shrinkage). For the third patient with a minor response (hepatocellular cancer, with maximum 5% tumor shrinkage), before progressing after 159 days (6 cycles), samples were not collected at all time points and hence a high acH3 signal could have been missed.

Discussion

SB939 is an inhibitor of class I, II, and IV HDACs, advanced into clinical trials because of its favorable pharmaceutical and pharmacokinetic properties (11); namely its oral availability and high distribution in tumor tissue, offering potential efficacy and safety advantages over other HDACi. To show target efficacy, a Western blot assay measuring acH3 on lysine 9 and 14 was developed, tested in cancer cell lines, PBMCs, and animal tumor models before being applied to PBMCs from patients in a phase I clinical trial (16).

The antibody used for the acH3 detection was raised against a peptide that is 100% identical in human and

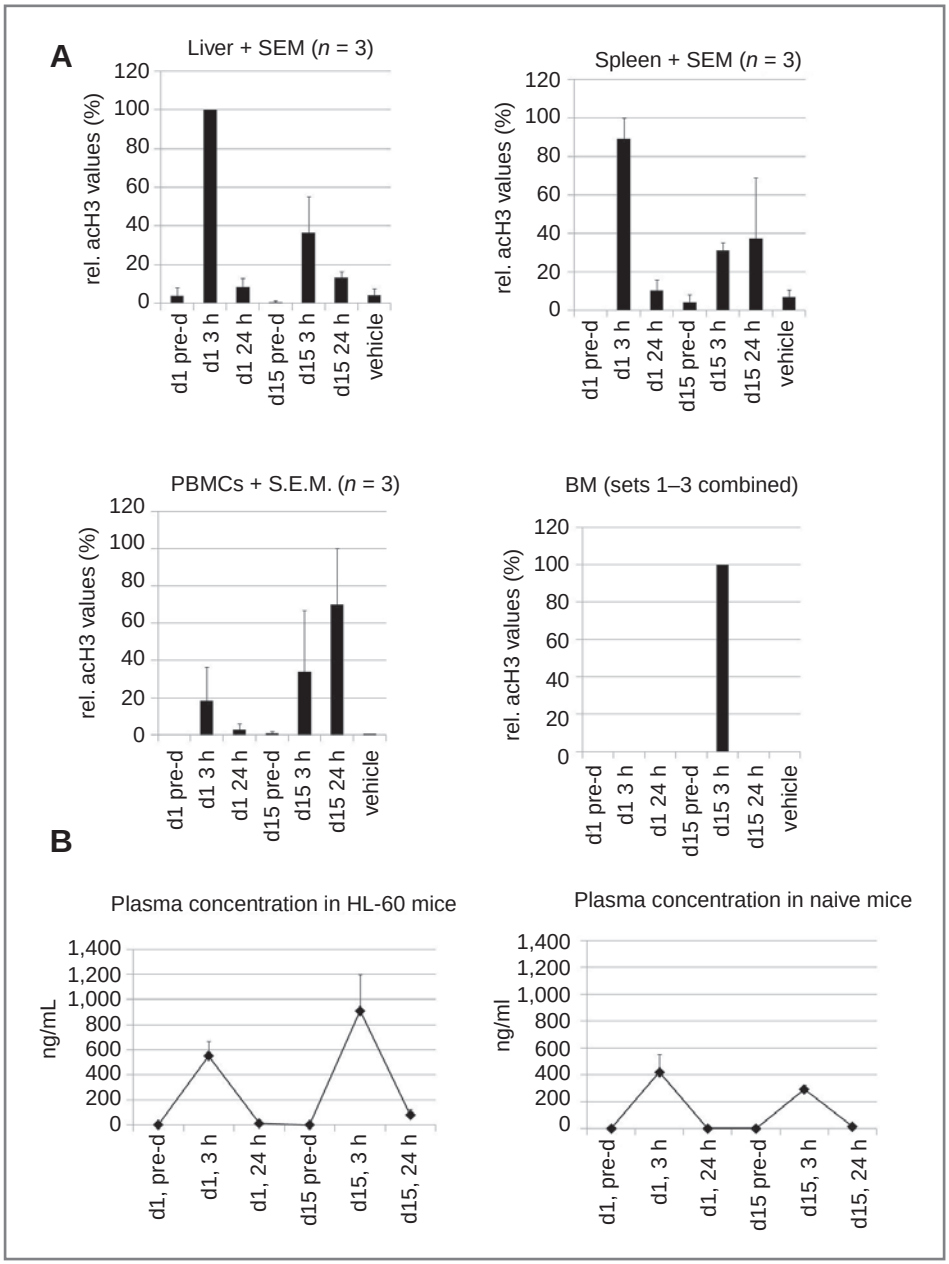

Figure 4. Acetylation of histone H3 increased in bone marrow and PBMCs of leukemic mice after prolonged treatment. SCID mice were injected i.v. with HL-60 cells and treated with 125 mg/kg SB939 3×/wk. A, animals were sacrificed at the indicated time points and tissues harvested and analyzed using Western blots. Graphs were prepared after densitometric analyses as described for Fig. 2 (+/− SEM), except for bone marrow, where 25 μg of tissue lysate from 3 different animals culled at each time point was added to a total loading of 75 μg, with the bar already representing an average of 3 animals. pre-d, predose; BM, bone marrow. B, SB939 plasma concentration of leukemic (HL-60) SCID mice from A (left), or naive SCID mice (right), $n = 3 \pm$ SD. pre-d, predose.

murine H3, recognizing human and murine acH3 equally (personal communication and V. Novotny-Diermayr, unpublished data) allowing validation of the assay in human and murine cells and tissues. Background signals in cells or tissues before exposure to SB939 were negligable, which is an important attribute as some antibodies previously used for HDAC target efficacy assays detected a signal before exposure of tissue to HDACi as published, for example, by Steele and colleagues after treatment with belinostat (17).

The concentration of SB939 detectable in this assay was 60 nmol/L (22 ng/mL, Fig. 1B), which was below the plasma drug levels measured at efficacious doses in animal tumor models as well as the C_{max} measured in patients from the lowest dose level (10 mg) in the phase I clinical trial (16), showing that the assay was sufficiently sensitive to be applied to measure target efficacy.

In tissues such as liver, spleen, and tumor from mice, there was little variation in the time postdose when maximal acH3 levels were measured, whereas signals obtained from murine PBMCs were more variable (see Figs. 2–5). One reason for this could be the lengthy isolation process necessary to obtain murine PBMCs, and the requirement to dilute samples 1:1 with PBS. Dilution is not required to isolate human PBMCs and the processing is faster, using CPT tubes, hence human

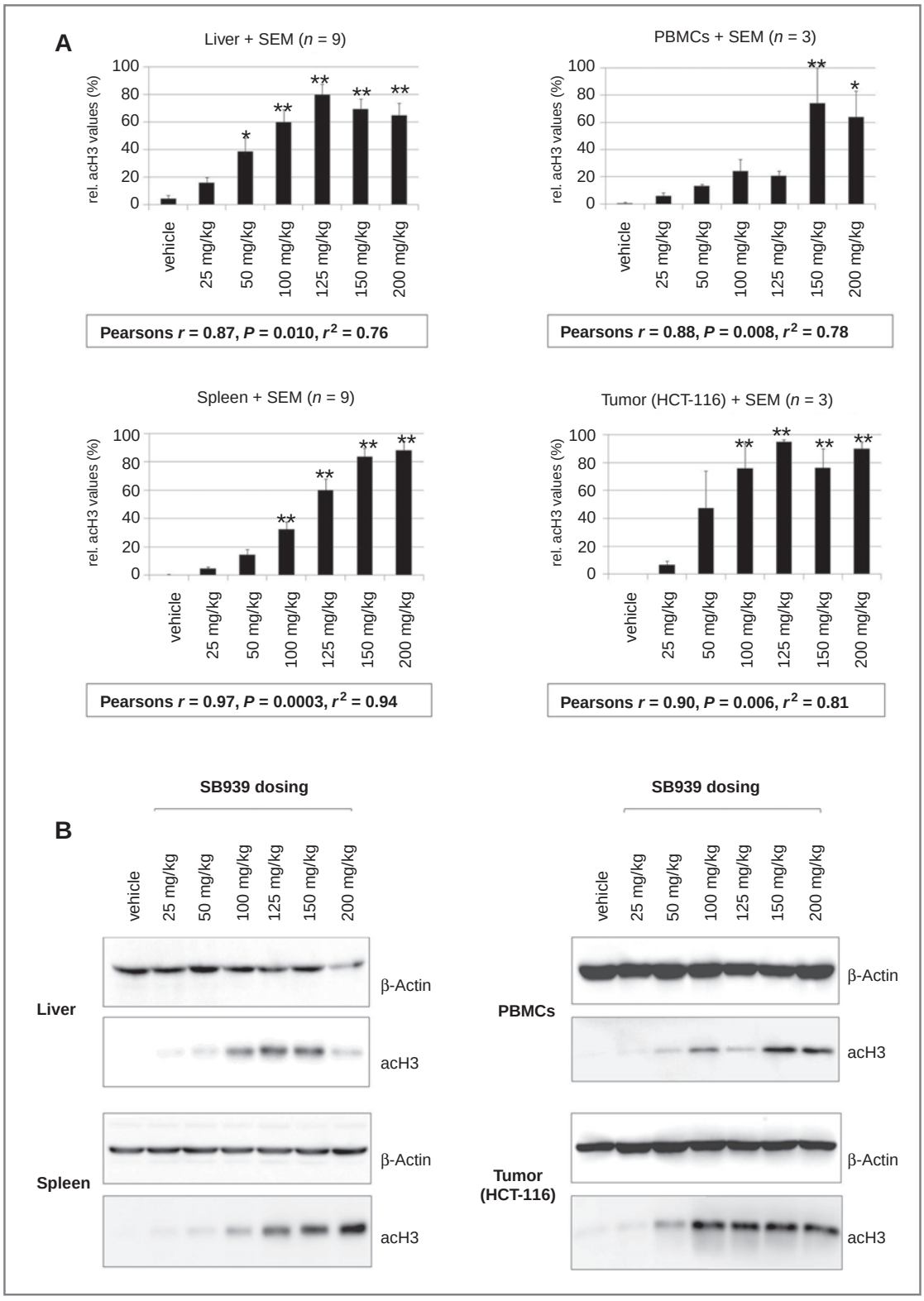

Figure 5. Acetylation of histone H3 increased dose dependently and correlated with the dose of SB939 administered. A, BALB/c mice or BALB/c nude mice were treated with the indicated amounts of SB939. Mice were sacrificed 3 hours postdose, tissues extracted, 25 μg of lysate subjected to Western blot analysis and the acH3/actin ratio determined. The highest value for each blot was set to be 100% to combine data from 3 (PBMCs, tumor) or 9 (other tissues) Western blots in 1 graph. *, $P < 0.05$, **, $P < 0.01$ by ANOVA Dunett's multiple comparison versus vehicle. B, 1 representative Western blot from each tissue from either HCT-116–xenografted nude mice (tumor, liver) or normal BALB/c mice (spleen, PBMCs) is shown.

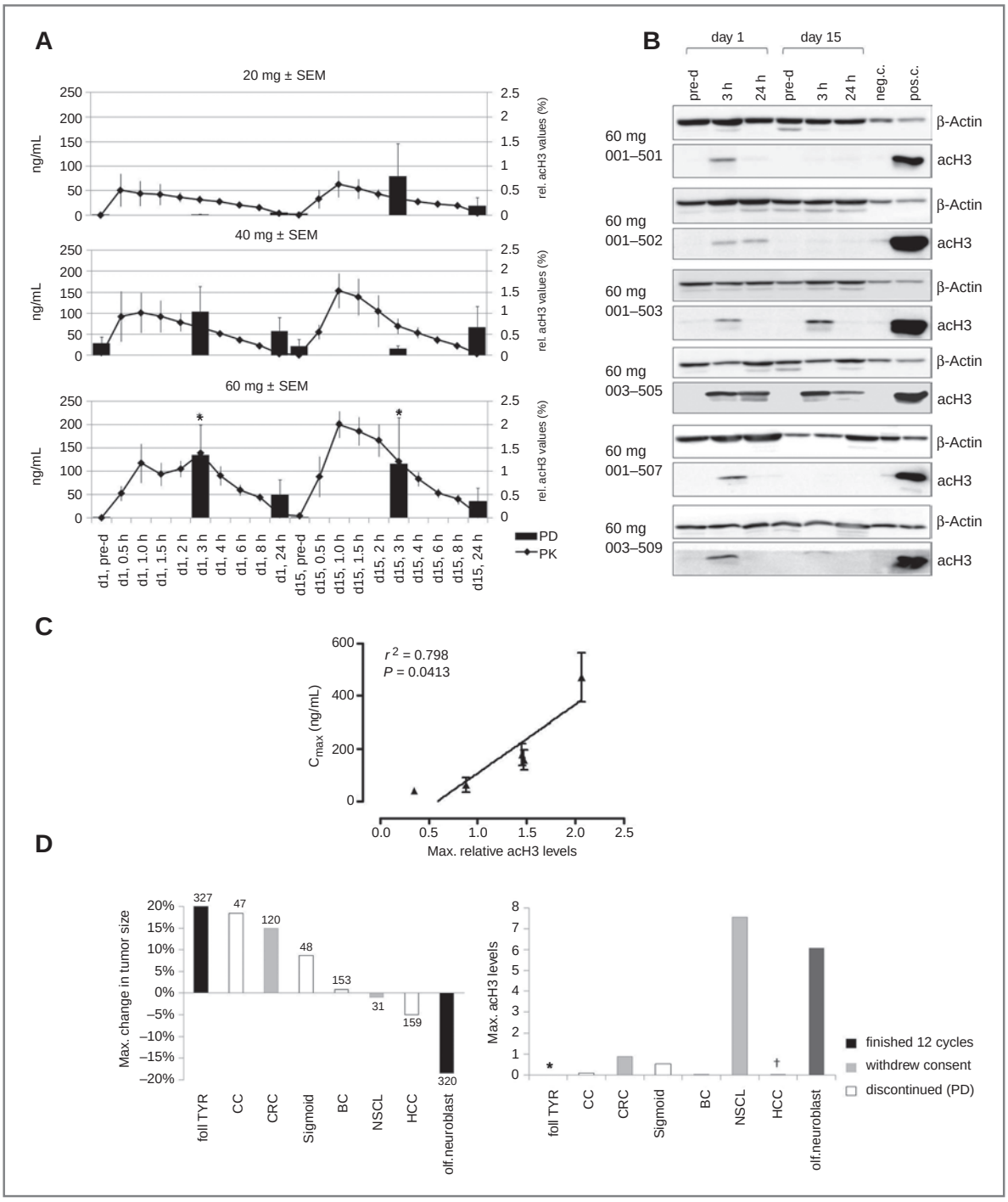

Figure 6. Correlations of the pharmacodynamic marker (acH3) with the pharmacokinetics of SB939 in plasma and clinical parameters in patient samples. A, PK-PD correlations: The left axis shows the SB939 plasma concentration in ng/mL at the time points indicated, the right axis shows the relative acH3 values. *, statistical significant difference of predose levels to the 3 hours postdose values ($P = 0.0265$). Patient n, given in the following format: (Dose level/PD[n]/PK [n]): 10 mg/$n = 2$/$n = 3$; 20 mg: $n = 3$, (except for day 15 predose, $n = 2$)/$n = 3$; 40 mg: $n = 8$ (day 1 predose and 3 hours) $n = 7$ (24 hours), day 15: $n = 5$/$n = 7$(d1) $n = 5$ (d15); 60 mg: day 1 $n = 8$, d15: $n = 6$/d1: $n = 9$, day 15: $n = 4$. B, Western blots of the complete samples ($n = 6$) for the 60 mg cohort; patient numbers indicated on the left, antibodies on the right. C, graphical analysis showing correlations between C_{max} and maximum relative acH3 levels (±SEM). D, left, maximum percentage change in tumor size (average of longest diameter in all target lesions) from all patients with a tumor size increase of 20% or less. Days on treatment given above/below the bars; the reasons for discontinuing treatment indicated on the right-hand side. D, right, maximum acH3 levels in the same patients. foll THYR, follicular thyroid carcinoma (80 mg); CC, colon cancer (80 mg); CRC, colorectal cancer (40 mg); Sigmoid, sigmoidal carcinoma (20 mg); BC, breast cancer (60 mg); NSCL, non–small cell lung cancer (80 mg); HCC, hepatocellular carcinoma (40 mg); olf. neuroblast, olfactory neuroblastoma (60 mg). *, relative acH3 values could not be obtained; †, relative acH3 values missing for some time points other than predose day 1.

PBMCs provide a more reliable surrogate tissue to evaluate pharmacodynamic response in solid tumor patients.

Interestingly, not all tissues responded to the same magnitude or duration. First, the various subpopulations of normal human PBMCs showed varying responses, with $CD20^+$ B-lymphocytes showing the strongest response and $CD16^+$ monocytic cells showing the lowest acH3 levels. Second, in animal models, the magnitude and duration of response were greater in tissues containing tumor cells compared with normal tissues, probably due to accumulation of drug in tumor tissue as observed previously (11). Therefore, although PBMCs could be used as surrogate tissue to measure the pharmacodynamic response in solid tumor patients, it will be difficult to study dose dependency of acH3 levels across liquid tumor patients, having variable numbers and types of circulating diseased cells. This is supported by the absence of published target efficacy biomarker studies using PBMCs of liquid tumor patients. The only data from leukemic patients were obtained using a quantitative flow-cytometric assay, gating for $CD34^+$ cells, hence looking only at a specific cell population, showing a significant increase of acH3 levels in 1 cohort compared with another without showing data for 3 other cohorts (14). Interestingly, the highest increase in acH3 was measured in $CD19^+$ B-cells, the same lineage we showed to have the strongest acH3 signal.

In preclinical models, acH3 in all tissues correlated with SB939 dose. When applied to PBMCs from 30 patients with advanced solid malignancies from the phase I trial, target efficacy was observed from the lowest dose level and the response was dose dependent across various doses tested (10–80 mg; ref. 16). In most patients, the induction of acH3 was strongest at the 3 hour time point on day 1, correlating with C_{max} and $AUC_{0-\infty}$ of SB939 in plasma. Such a clear relationship between pharmacokinetic and pharmacodynamics was not shown for other HDACi in clinical trials. Mocetinostat was shown to increase HDAC activity in a whole cell enzyme assay (13, 18) and vorinostat showed a trend toward a dose-dependent increase of acH3 in histone extracts from solid tumors, measured by ELISA (12).

Efforts are currently being made to identify predictive biomarkers for response to HDACi treatment (4, 19, 20). Intriguingly, 2/3 patients with a minor tumor response were also the patients with the strongest acH3 signals, raising speculation that relative high induction of acH3 in response to therapy might predict a good patient outcome. However, this interesting observation requires evaluation in a much larger patient population for confirmation.

Using histone acetylation as a pharmacodynamic biomarker, we showed that the favorable pharmacokinetic and pharmacodynamic properties of SB939 translated from preclinical models to patients.

Disclosure of Potential Conflicts of Interest

V. Novotny-Diermayr, N. Sausgruber, Y.K. Loh, M.K. Pasha, R. Jayaraman, H. Hentze, K. Ethirajulu, J. Zhu and J.M. Wood are employees of S*BIO Pte. Ltd. V. Novotny-Diermayr also has ownership interests, including patents from S*BIO.

Acknowledgment

We would like to acknowledge Albert Cheong, Vasantha Nayagam, and Ai Leng Liang for their excellent technical help during this project.

The costs of publication of this article were defrayed in part by the payment of page charges. This article must therefore be hereby marked *advertisement* in accordance with 18 U.S.C. Section 1734 solely to indicate this fact.

Received January 19, 2011; revised May 10, 2011; accepted May 11, 2011; published OnlineFirst May 17, 2011.

References

1. Haberland M, Montgomery RL, Olson EN. The many roles of histone deacetylases in development and physiology: implications for disease and therapy. Nat Rev Genet 2009;10:32–42.
2. Glozak MA, Sengupta N, Zhang X, Seto E. Acetylation and deacetylation of non-histone proteins. Gene 2005;363:15–23.
3. Marks P, Rifkind RA, Richon VM, Breslow R, Miller T, Kelly WK. Histone deacetylases and cancer: causes and therapies. Nat Rev Cancer 2001;1:194–202.
4. Stimson L, La Thangue NB. Biomarkers for predicting clinical responses to HDAC inhibitors. Cancer Lett 2009;280:177–83.
5. Timmermann S, Lehrmann H, Polesskaya A, Harel-Bellan A. Histone acetylation and disease. Cell Mol Life Sci 2001;58:728–36.
6. Dokmanovic M, Clarke C, Marks PA. Histone deacetylase inhibitors: overview and perspectives. Mol Cancer Res 2007 Oct;5:981–9.
7. Carew JS, Giles FJ, Nawrocki ST. Histone deacetylase inhibitors: mechanisms of cell death and promise in combination cancer therapy. Cancer Lett 2008;269:7–17.
8. Duvic M, Vu J. Vorinostat: a new oral histone deacetylase inhibitor approved for cutaneous T-cell lymphoma. Expert Opin Investig Drugs 2007;16:1111–20.
9. Campas-Moya C. Romidepsin for the treatment of cutaneous T-cell lymphoma. Drugs Today (Barc) 2009;45:787–95.
10. Lee MJ, Kim YS, Kummar S, Giaccone G, Trepel JB. Histone deacetylase inhibitors in cancer therapy. Curr Opin Oncol 2008;20:639–49.
11. Novotny-Diermayr V, Sangthongpitag K, Hu CY, Wu X, Sausgruber N, Yeo P, et al. SB939, a novel potent and orally active histone deacetylase inhibitor with high tumor exposure and efficacy in mouse models of colorectal cancer. Mol Cancer Ther 2010;9:642–52.
12. Kelly WK, O'Connor OA, Krug LM, Chiao JH, Heaney M, Curley T, et al. Phase I study of an oral histone deacetylase inhibitor, suberoylanilide hydroxamic acid, in patients with advanced cancer. J Clin Oncol 2005;23:3923–31.
13. Bonfils C, Kalita A, Dubay M, Siu LL, Carducci MA, Reid G, et al. Evaluation of the pharmacodynamic effects of MGCD0103 from preclinical models to human using a novel HDAC enzyme assay. Clin Cancer Res 2008;14:3441–9.
14. Giles F, Fischer T, Cortes J, Garcia-Manero G, Beck J, Ravandi F, et al. A phase I study of intravenous LBH589, a novel cinnamic hydroxamic acid analogue histone deacetylase inhibitor, in patients with refractory hematologic malignancies. Clin Cancer Res 2006;12:4628–35.
15. Ryan QC, Headlee D, Acharya M, Sparreboom A, Trepel JB, Ye J, et al. Phase I and pharmacokinetic study of MS-275, a histone deacetylase inhibitor, in patients with advanced and refractory solid tumors or lymphoma. J Clin Oncol 2005;23:3912–22.
16. Yong WP, Goh BC, Soo R, Toh HC, Ethirajulu K, Wood J, et al. Phase I and pharmacodynamic study of an orally administered novel inhibitor of histone deacetylases, SB939, in patients with refractory solid malignancies. Ann Oncol 2011; in press.

17. Steele NL, Plumb JA, Vidal L, Tjornelund J, Knoblauch P, Rasmussen A, et al. A phase 1 pharmacokinetic and pharmacodynamic study of the histone deacetylase inhibitor belinostat in patients with advanced solid tumors. Clin Cancer Res 2008;14:804–10.
18. Siu LL, Pili R, Duran I, Messersmith WA, Chen EX, Sullivan R, et al. Phase I study of MGCD0103 given as a three-times-per-week oral dose in patients with advanced solid tumors. J Clin Oncol 2008;26:1940–7.
19. Fotheringham S, Epping MT, Stimson L, Khan O, Wood V, Pezzella F, et al. Genome-wide loss-of-function screen reveals an important role for the proteasome in HDAC inhibitor-induced apoptosis. Cancer Cell 2009;15:57–66.
20. Khan O, Fotheringham S, Wood V, Stimson L, Zhang C, Pezzella F, et al. HR23B is a biomarker for tumor sensitivity to HDAC inhibitor-based therapy. Proc Natl Acad Sci USA ;107:6532–7.